Biosensors Hot Paper

How to cite:
International Edition: doi.org/10.1002/anie.202101731
German Edition: doi.org/10.1002/ange.202101731

A Ratiometric Fluorescent Biosensor Reveals Dynamic Regulation of Long-Chain Fatty Acyl-CoA Esters Metabolism

Weibo Wang[+], Qingpeng Wei[+], Jiayuan Zhang, Meiqi Zhang, Chuchen Wang, Renyu Qu, Yuan Wang, Guangfu Yang, and Jing Wang**

Abstract: *Despite increasing awareness of the biological impacts of long-chain fatty acyl-CoA esters (LCACoAs), our knowledge about the subcellular distribution and regulatory functions of these acyl-CoA molecules is limited by a lack of methods for detecting LCACoAs in living cells. Here, we report development of a genetically encoded fluorescent sensor that enables ratiometric quantification of LCACoAs in living cells and subcellular compartments. We demonstrate how this FadR-cpYFP fusion "LACSer sensor" undergoes LCACoA-induced conformational changes reflected in easily detectable fluorescence responses, and show proof-of-concept for real-time monitoring of LCACoAs in human cells. Subsequently, we applied LACSer in scientific studies investigating how disruption of ACSL enzymes differentially reduces cytosolic and mitochondrial LCACoA levels, and show how genetic disruption of an acyl-CoA binding protein (ACBP) alters mitochondrial accumulation of LCACoAs.*

Introduction

Long-chain fatty acyl-CoA esters (LCACoAs, acyl chain >12 carbons) are amphipathic molecules composed of a hydrophilic coenzyme A and a hydrophobic acyl chain. Currently, LCACoAs are understood as intermediates in lipid biosynthesis and fatty acid degradation.[1] These molecules are involved in the biosynthesis of glycerides,[2] sphingomyelin,[3] and very long-chain fatty acids,[4] thereby influencing lipid levels in cells. Discoveries in recent years have helped widen the appreciation of the wider range of impacts from LCACoAs in biological processes, including for example on gene expression,[5] enzyme activity,[6] vesicle fusion,[7] insulin secretion,[8] and ion channel transport dynamics.[9] Biochemically, it is now clear how the role of LCACoAs in cells affect the class of posttranslational modifications referred to collectively as protein lipidation.[10] Such lipidation includes myristoylation and palmitoylation among others,[11] and studies have confirmed the requirement for the palmitoylation or myristoylation of particular proteins in diverse biological processes such as signal transduction,[12] immune activation,[13] cellular differentiation and apoptosis,[14] and more broadly in the dynamic regulation of protein functions in response to both intrinsic and extrinsic clues.[15] Furthermore, many recent oncology studies have found that LCACoAs are closely associated to the viability and proliferation of tumor cells, as well as to tumorigenesis and metastasis.[16]

The intracellular concentration of LCACoAs is controlled by the activities of acyl-CoA thioesterase (ACOT)[17] and long-chain acyl-CoA synthetases (ACSLs),[18] as well as the cellular acyl-CoA binding proteins (ACBP).[19] Of note, LCACoAs are highly compartmentalized in cells.[20] So, although we know that their concentrations and particular subcellular distributions strongly impact cells and compartment-specific metabolism, currently available bioanalytic technologies are unable to support real-time monitoring of LCACoAs and do not support spatially resolved in vivo analyses. Traditional chromatographic methods can achieve the quantitative detection of LCACoAs in subcellular organelles,[21] but subcellular fractionation is inherently destructive and is not conducted in real-time. Thus, methods that support spatiotemporal tracking of LCACoAs metabolism in living cells could substantially deepen our understanding of both LCACoAs biochemistry and of the apparently widespread impacts of these metabolites on cells and disease.

Here, we report the development of an innovative genetically encoded fluorescent sensor that enables the direct, rapid, sensitive, and specific detection LCACoAs in living cells and subcellular compartments. The sensor was engineered by coupling a conformation sensitive circular-permutated YFP (cpYFP)[22] with an *E. coli* protein known to bind LCACoAs. After iterative engineering and optimization of our LACSer (long-chain acyl-CoA sensor) system, we conducted extensive in vitro and in vivo assays in human cells. We demonstrate that LACSer's affinity for LCACoAs and its sensitive and easily detectable fluorescence responses realize real-time monitoring of the spatiotemporal distribution and dynamic changes of LCACoAs. Subsequently, we successfully

[*] W. B. Wang,[+] Q. P. Wei,[+] M. Q. Zhang, C. C. Wang, Y. Wang, Prof. J. Wang
State Key Laboratory of Natural and Biomimetic Drugs
Department of Chemical Biology
School of Pharmaceutical Sciences, Peking University
Beijing 100191 (China)
E-mail: wangjingsioc@pku.edu.cn

W. B. Wang,[+] R. Y. Qu, Prof. G. F. Yang
Key Laboratory of Pesticide & Chemical Biology of Ministry of Education, International Joint Research Center for Intelligent Biosensor Technology and Health, College of Chemistry
Central China Normal University, Wuhan 430079 (China)
E-mail: gfyang@mail.ccnu.edu.cn

J. Y. Zhang
Wellcome Centre for Human Genetics, University of Oxford
Roosevelt Dr, Headington, Oxford OX3 7BN (UK)

[+] These authors contributed equally to this work.

Supporting information and the ORCID identification number(s) for the author(s) of this article can be found under: https://doi.org/10.1002/anie.202101731.

These are not the final page numbers!

applied LACSer in two scientific investigations, exploring i) how chemical and genetic disruption of ACSL function reduces LCACoA levels in real-time and ii) how the rate of mitochondria-specific LCACoAs utilization differs from the rate of cytosolic LCACoAs utilization upon such disruption of ACBP function.

Results and Discussion

A transcription factor from bacteria, FadR, has been reported[23] to bind LCACoAs, and such binding inhibits its capacity to interact with DNA. The known K_d values of FadR to myristoyl-CoA (C14:0), palmitoyl-CoA (C16:0), and oleoyl-CoA (C18:1) are 59, 369, and 63 nM, respectively,[23] indicating that FadR is apparently able to bind, with high affinity, to acyl-CoA molecules containing an acyl chain longer than C14:0. Structural studies based on a crystal structure of FadR showed that the binding of myristoyl-CoA (C14:0) induces conformational changes of the protein, specifically at Met168 and Tyr172 and at the hinge region (Figure 1a), with backbone shifts up to 4.5 Å.[24] Subsequently, the difference in the Cα dihedral angle between unbound and myristoyl-CoA-bound states of FadR was explored through further computational calculations, as this difference should be indicative of the magnitude of local conformational changes around certain amino acid residues.[25] This analysis implicated Leu89 and His91 in the FadR hinge region as apparent hotspots for large conformation changes (Figure 1b). Thus, based on the characteristics of high affinity for LCACoAs and conformational changes, FadR may suitable for developing proteinaceous sensors.

Next, we considered and initially explored possible methods to generate LCACoAs sensor. We started with FadR as the sensing module and coupled it to a circularly permuted yellow fluorescent protein (cpYFP), which was originally reported[22] as part of a hydrogen peroxide sensor (HyPer) as a fluorescent light output module (Figure 1c). We hypothesized that upon LCACoAs binding, the conformational changes of transcription factor could alter the arrangement of the associated cpYFP, resulting in a LCACoA-dependent change in fluorescence. We constructed five chimeras in which cpYFP was inserted into the hinge region and binding pocket of FadR. All five fusion proteins expressed in *E. coli* were fluorescent, while only the variant with cpYFP at His91 showed a significant change of fluorescence in the presence of myristoyl-CoA (C14:0) (Figure 1d).

Subsequently, we used a two-step approach to engineer FadR-cpYFP, to improve the performance of the sensor. First, we conducted site mutations on the residues near the binding

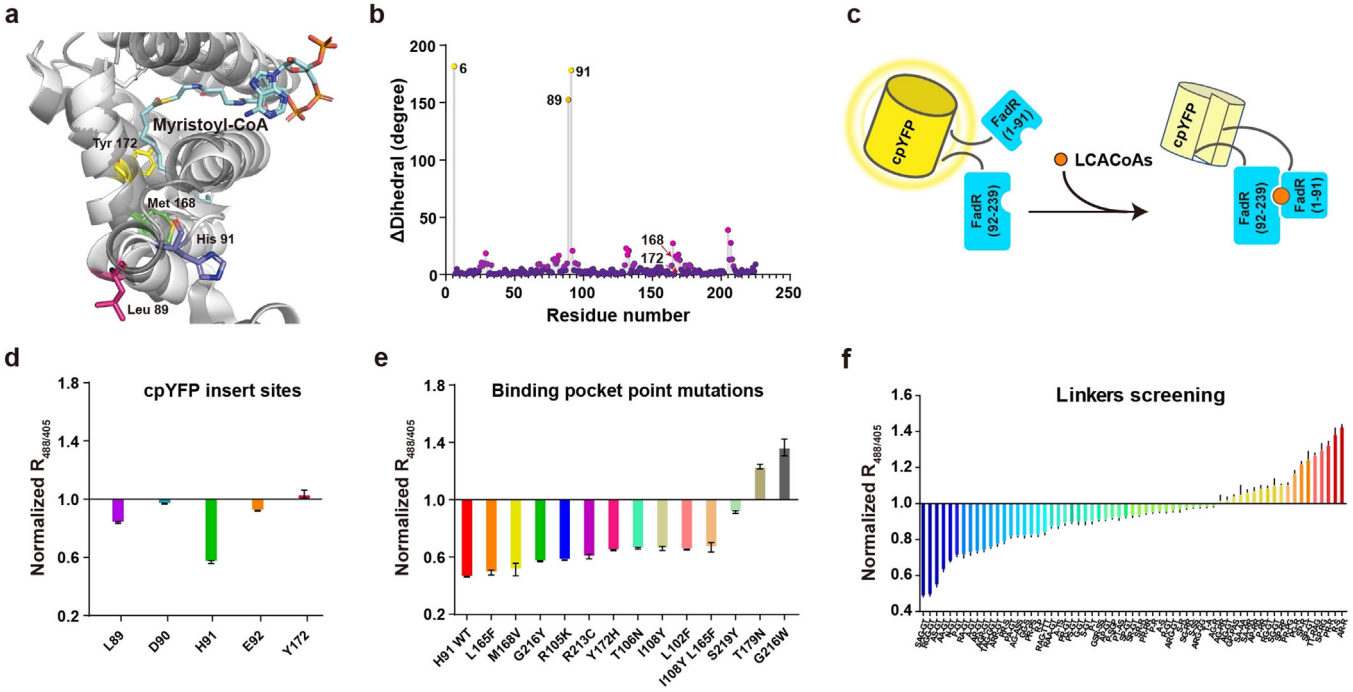

Figure 1. Design and construction of the LCACoAs sensor LACSer. a) The crystal structure using the closed form of FadR (1h9g, white) bound to myristoyl-CoA and the open form of FadR (without a ligand) (1hw1, gray) indicates the magnitude of the local conformational changes. b) The difference in Cα dihedrals between apo and myristoyl-CoA-bound state of FadR plotted against residue number (*n*). The Cα dihedrals were calculated from the coordinates of $C\alpha_{n-1}$, $C\alpha_n$, $C\alpha_{n+1}$, $C\alpha_{n+2}$ and corrected to fall within a range of 0–180°. c) Schematic showing the design to generate a LCACoAs fluorescent biosensor. The design of LACSer, which is a complete fusion of a FadR monomer and cpYFP. The fluorescent protein cpYFP is inserted into the region where FadR undergoes the largest conformational change. d) Fluorescence response of different FadR-cpYFP fusion proteins to 12.5 μM myristoyl-CoA denoted by name and number of the residue after which cpYFP was inserted. e) Fluorescence response of thirteen variants in the presence of 12.5 μM palmitoyl-CoA. f) Screening result of 63 linker variants. Blue to red vertical bars indicate fluorescence response in the presence of 12.5 μM palmitoyl-CoA. In (d)–(f), each bar represents the mean of three replicates and the error bars indicate the SEM.

pocket,[24] but no variants performed better than the original FadR-cpYFP backbone (Figure 1e). Second, we optimized the linker[26] residues between cpYFP and FadR. After screening 63 variants, no variants superior to the original linker pair were found (Figure 1f). Thus, we still selected the original linker consisting of the N-terminal Ser-Ala-Gly linker and the C-terminal Gly-Thr linker to further characterize the variant, which we termed LACSer (long-chain acyl-CoA sensor).

To further characterize the fluorescence response of LACSer to LCACoAs, we purified LACSer and tested its fluorescence response under various conditions, using purified cpYFP as a negative control (Supporting Information, Figure S1a and S1b). The sensor has typical excitation and emission spectra of other cpYFP-based genetically encoded sensors,[27] with two excitation peaks around 405 nm and 488 nm and one emission peak at 517 nm. LACSer exhibited obvious decreases in fluorescence with excitation at 488 nm upon palmitoyl-CoA (C16:0), myristoyl-CoA (C14:0) or oleoyl-CoA (C18:1) binding, and a second excitation peak at 405 nm was slightly increased, resulting in a larger change in the emission intensity ratio between 488 nm and 405 nm excitation ($R_{488/405}$) (Figure 2a). This ratiometric change allows us to normalize the signal and correct for changes in sensor levels by measuring the ratio of the fluorescence at two wavelengths (Figure S2a–f).

We also found that incubation of myristoyl-CoA, palmitoyl-CoA, or oleoyl-CoA with purified LACSer resulted in a decrease in $R_{488/405}$ signal, and these decreases were dose-dependent (Figure S3a, S3c and S3e); in contrast, incubation with these LCACoAs only minimally affected cpYFP fluorescence (Figure S3b, S3d and S3f). Further fluorescence titration studies showed that LACSer has apparent Kd values for myristoyl-CoA, palmitoyl-CoA, and oleoyl-CoA of 657, 322, and 450 nM, respectively (Figure 2b).

To determine the specificity of LACSer sensor, we evaluated the fluorescence response in the presence of acyl-CoA with different chain lengths. LACSer only displayed a significant fluorescence response to LCACoAs; i.e., no detectable fluorescence changes were evident upon addition

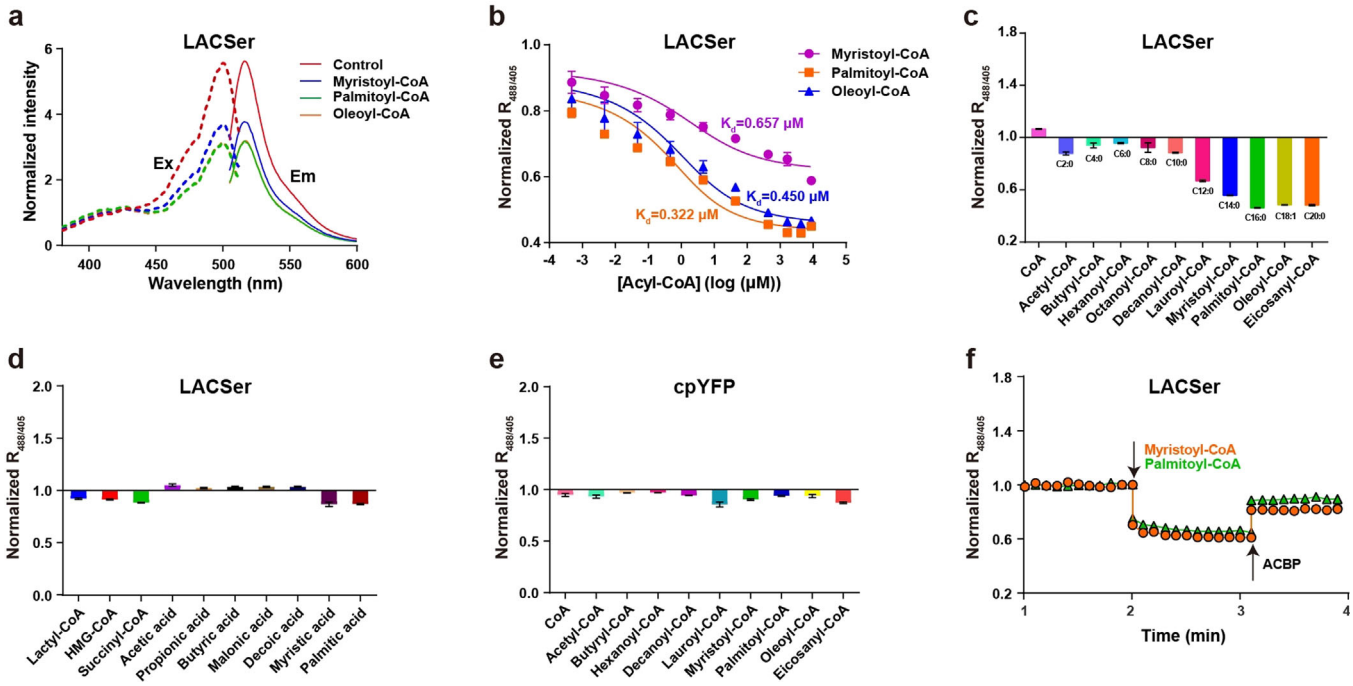

Figure 2. Properties of the genetically encoded LCACoAs sensor LACSer. a) Fluorescence spectra of purified LACSer. Excitation (Ex, dashed lines) and emission (Em, solid lines) scans of the purified sensor with either 0 (red) or 12.5 µM myristoyl-CoA (blue), palmitoyl-CoA (green), or oleoyl-CoA (orange); excitation was monitored at 517 nm, and emission was monitored after excitation at 500 nm. Data are normalized to peak intensity at 420 nm in the control condition. b) Dose-response curves for purified LACSer for multiple LCACoA analytes. The ratio of fluorescence intensities upon excitation at 488 nm, divided by 405 nm ($R_{488/405}$) upon addition of myristoyl-CoA (C14:0), palmitoyl-CoA (C16:0), or oleoyl-CoA (C18:1) to the assay solution. c, d) Specificity of LACSer. The ratio of fluorescence intensities upon excitation at 488 nm divided by 405 nm ($R_{488/405}$) in the presence of LCACoAs (each of 12.5 µM myristoyl-CoA, palmitoyl-CoA, oleoyl-CoA, and eicosanyl-CoA) and the seven indicated synthetic structural analogs (each of 100 µM CoA, acetyl-CoA (C2:0), butyryl-CoA (C4:0), hexanoyl-CoA (C6:0), and octanoyl-CoA (C8:0); each of 12.5 µM decanoyl-CoA (C10:0), and lauroyl-CoA (C12:0)) (c). The ratio of fluorescence intensities upon excitation at 488 nm divided by 405 nm ($R_{488/405}$) in the presence of special structure acyl-CoA (each of 100 µM lactyl-CoA, succinyl-CoA, and HMG-CoA) and the seven indicated fatty acids (each of 1 mM acetic acid, propionic acid, butyric acid, malonic acid; each of 0.1 mM decoic acid, myristic acid, and palmitic acid) (d). e) Specificity of cpYFP. The ratio of fluorescence intensities upon excitation at 488 nm divided by 405 nm ($R_{488/405}$) in the presence of LCACoAs (each of 200 µM myristoyl-CoA, palmitoyl-CoA, oleoyl-CoA, and eicosanyl-CoA) and the six indicated synthetic structural analogs (each of 200 µM CoA, acetyl-CoA (C2:0), butyryl-CoA (C4:0), hexanoyl-CoA (C6:0), decanoyl-CoA (C10:0), and lauroyl-CoA (C12:0)). f) Kinetics of fluorescence response of purified LACSer protein to 5 µM myristoyl-CoA or 5 µM palmitoyl-CoA, respectively. Addition of 8 µM acyl-CoA binding protein (ACBP) to compete with LACSer for binding to myristoyl-CoA or palmitoyl-CoA. In (b)–(f), data represent the mean of three replicates and the error bars indicate the SEM.

of short-chain (C2-C6) or medium-chain (C8-C10) acyl-CoA molecules (Figure 2c). Nor were detectable fluorescence changes evident upon addition of lactyl-CoA, succinyl-CoA, HMG-CoA (3-hydroxy-3-methylglutaryl-CoA), or fatty acids (Figure 2d). We also tested the fluorescence changes of purified cpYFP: in the presence of acyl-CoA, cpYFP does not display any obvious fluorescence changes, suggesting that the fluorescence change was not caused by the perturbation of the chromophore (Figure 2e). Taken together, these results demonstrate that the LACSer sensor has excellent specificity for LCACoAs.

Like other cpFP-based sensors, the LACSer fluorescence may be sensitive to pH.[28] Briefly, our analyses of LACSer and cpYFP fluorescence at pH values ranging between 6.8 and 8.0 showed that, in the absence of LCACoAs, LACSer and cpYFP displayed very similar sensitivities to pH (Figure S4a and S4b). Accordingly, impacts from pH can be corrected by normalizing LACSer fluorescence based on data for cpYFP fluorescence as measured in parallel experiments (Figure S4c).[29] LACSer can sense LCACoAs such as myristoyl-CoA, palmitoyl-CoA, or oleoyl-CoA in the physiologically relevant pH range of 7.0–8.0, with the maximum response of the $R_{488/405}$ signal for LCACoAs only marginally affected by the tested elevated pH conditions (Figure S4d–f). Moreover, the fluorescence response of LACSer to myristoyl-CoA, palmitoyl-CoA, and oleoyl-CoA was not appreciably affected by temperature between 25° and 35° (Figure S4g–i).

We also monitored LACSer fluorescence in real time in the presence of acyl-CoA binding protein (ACBP), which has a higher affinity for LCACoAs ($K_d \approx 1$–10 nM)[19] than LACSer does, meaning it should outcompete LACSer for binding with free LCACoAs. We observed that LACSer fluorescence decreased rapidly in the presence of myristoyl-CoA and palmitoyl-CoA, and the fluorescence recovered rapidly upon ACBP addition (Figure 2f). These results demonstrate the reversibility of the fluorescence output upon LACSer-substrate binding, supporting its application for real-time measurement applications.

To evaluate the utility of LACSer for evaluation of fluctuations in the intracellular concentrations of LCACoAs, we expressed the LACSer sensor in HEK293T cells for further testing. The gene for the fusion sensor construct was expressed in one of two forms: without any targeting peptide (for cytoplasmic localization: "LACSer") or with four N-terminal copies of a mitochondrial-targeting sequence (for mitochondrial localization: "mito-LACSer"). We found that LACSer exhibited strong fluorescence in the cytoplasm and that mito-LACSer exhibited strong fluorescence in mitochondria (Figure S5a and S5b). We also used immunoblotting to assess the cytoplasmic and mitochondrial expression levels of LACSer and mito-LACSer (Figure S5c and S5d).

Since LCACoAs cannot be transported across the cell plasma membrane,[30] our experiments testing intracellular levels of LCACoAs required use of a cell permeabilization agent (e.g., digitonin). We first used propidium iodide to assess the permeability of digitonin in HEK293T cells, and confirmed that the concentration of digitonin was in the range of 10–15 μM (Figure S6a and S6b). Next, we added palmitoyl-CoA to permeabilized HEK293T cells and extracted the LCACoAs for quantitative analysis by HPLC-MS. The exogenous additional palmitoyl-CoA indeed increased the levels of palmitoyl-CoA in HEK293T cells, doing so in a dose-dependent manner (Figure S6c). We also confirmed that digitonin does not affect the fluorescence response of the sensor in vitro or in the HEK293T cells (Figure S6d and S6e). For HEK293T cells expressing LACSer the addition of 5 μM each of myristoyl-CoA, palmitoyl-CoA, and oleoyl-CoA each caused immediate decreases in fluorescence ratio (by approximately 20%); no such decrease was detected in control cells expressing free cpYFP (Figure 3a–f and Figure S7a). These results demonstrate that our LACSer sensor can perceive and report fluctuations in LCACoA concentrations when expressed in living cells.

To test the specificity of LACSer in living cells, we treated the cells expressing LACSer with short-chain acyl-CoA or other structurally diverse acyl-CoA molecules following digitonin permeabilization. In the presence of butyryl-CoA (C4:0), HMG-CoA, or lactyl-CoA, no LACSer fluorescence response was detected by confocal microscopy (Figure 3g–l and Figure S7b). Collectively, these results confirm that our LACSer sensor can distinguish LCACoAs from structurally related analogs.

Then we turned our attention to investigate the dynamic production and consumption of endogenous LCACoAs inside cells. Long chain acyl-CoA synthetases (ACSLs) catalyze the covalent ligation of long chain fatty acids (FA, C12-C20) with coenzyme A (CoA) to generate LCACoAs.[18] In addition to controlling the metabolic fate of FAs, ACSLs also regulate the intracellular pools of FAs and LCACoAs,[31] which have a wide range of effects on cellular metabolism.

To empirically determine the influence of ACSLs on intracellular LCACoA levels, we treated HEK293T cells expressing LACSer or cpYFP with Triacsin C, an competitive inhibitor of ACSLs[32] (Figure S8a) and monitored the $R_{488/405}$ fluorescence signal via confocal microscopy. The fluorescence signal increased by about 30% within 20 minutes of Triacsin C addition, results indicating that the cellular LCACoA levels decreased; the fluorescence ratio for free cpYFP was unaltered by the presence of Triacsin C (Figure 4a,b and Figure S8b), thus excluding the possibility of interference of fluorescence emission due to pH variation. In addition, a reported covalent inhibitor of ACSLs, N-ethylmaleimide (NEM)[32] (Figure S8c), was used to treat HEK293T cells: we similarly observed an increase in the $R_{488/405}$ fluorescent signal of LACSer (Figure 4c and Figure S8d), reflecting a reduction in the cellular LCACoA levels. Further, we determined that the LACSer fluorescence response in these cells was inhibitor-dose-dependent (Figure S8e). Notably, we detected a decreased fluorescence in cpYFP-expressing HEK293T cells upon addition of a high concentration of NEM (5 mM) (Figure 4c and d), suggesting a slight decrease in pH during the 30 min time course. To correct for NEM-mediated effects on pH in our LCACoAs measurements, we normalized the LACSer fluorescence based on the cpYFP fluorescence signal measured in parallel experiments (Figure 4d).[29] We again used HPLC-MS to evaluate the effects of Triacsin C or NEM on the intracellular acyl-CoA levels. Both of the ACSL inhibitors significantly decreased LCACoA levels in

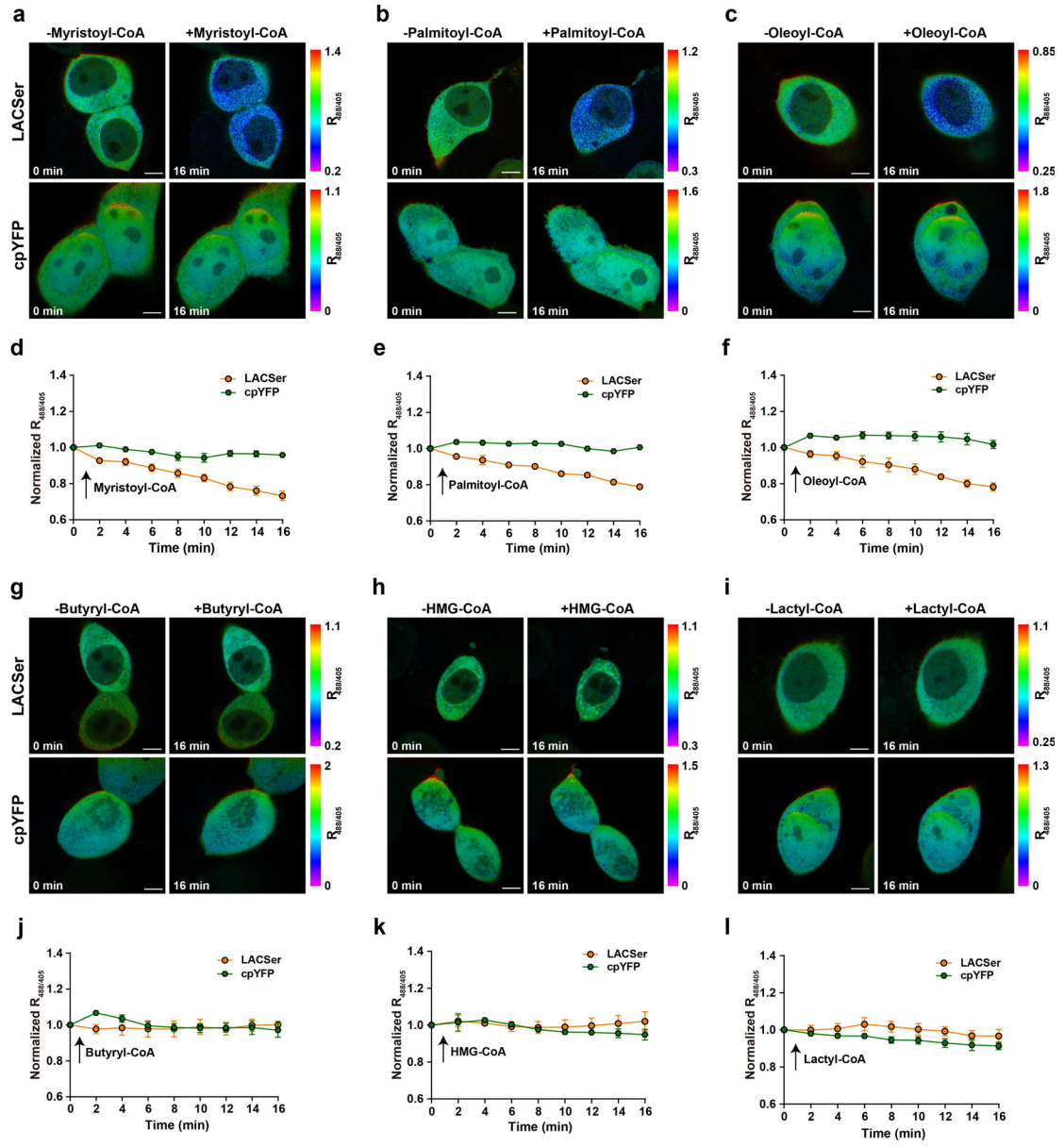

Figure 3. Dynamic detection of LCACoAs in mammalian cells. a–f) Fluorescent images (upper panels, a–c) and time course of $R_{488/405}$ fluorescent signal changes (lower panels, d–f) of permeabilized HEK293T cells expressing LACSer or free cpYFP in response to 5 μM myristoyl-CoA (a), palmitoyl-CoA (b), or oleoyl-CoA (c). For fluorescent images, the experiment was repeated with three cultures; similar results were obtained each time. Scale bar: 5 μm. For the time course of $R_{488/405}$ fluorescence signal changes, data are presented as the mean ± SEM (LACSer: $n=4$ cells from three cultures; cpYFP: $n=4$ cells from three cultures (d), LACSer: $n=5$ cells from three cultures; cpYFP: $n=6$ cells from three cultures (e), LACSer: $n=4$ cells from three cultures; cpYFP: $n=4$ cells from three cultures (f)). g–l) Fluorescent images (upper panels, g–i) and time course of $R_{488/405}$ fluorescent signal changes (lower panels, j–l) of permeabilized HEK293T cells expressing LACSer or free cpYFP in response to 20 μM butyryl-CoA (g), HMG-CoA (h) or lactyl-CoA (i). For fluorescent images, the experiment was repeated with three cultures; similar results were obtained each time. Scale bar: 5 μm. For the time course of $R_{488/405}$ fluorescence signal change, data are presented as the mean ± SEM (LACSer: $n=4$ cells from three cultures; cpYFP: $n=4$ cells from three cultures (j), LACSer: $n=3$ cells from three cultures; cpYFP: $n=6$ cells from three cultures (k), LACSer: $n=4$ cells from three cultures; cpYFP: $n=4$ cells from three cultures (l)). The LACSer signal is presented as a pixel-by-pixel ratio between the 488 nm excitation image and the 405 nm excitation image.

HEK293T cells (Figure S9a and S9b). In addition, no obvious fluorescence response was observed when we added Triacsin C or NEM to purified LACSer or cpYFP (Figure S9c–f), excluding the possibility that the observed fluorescence response resulted from a direct physical interaction between the inhibitors and LACSer or cpYFP. These results collectively demonstrate that LACSer can sense and report fluctuations in LCACoA levels in cells in real time.

Having demonstrated proof-of-concept for LACSer's real-time in vivo detection of altered LCACoA metabolism upon chemical inhibition of ACSLs, we next conducted knockdown studies using siRNAs to specifically knock down ACSL3 in HEK293T cells (Figure 4e). As expected, when

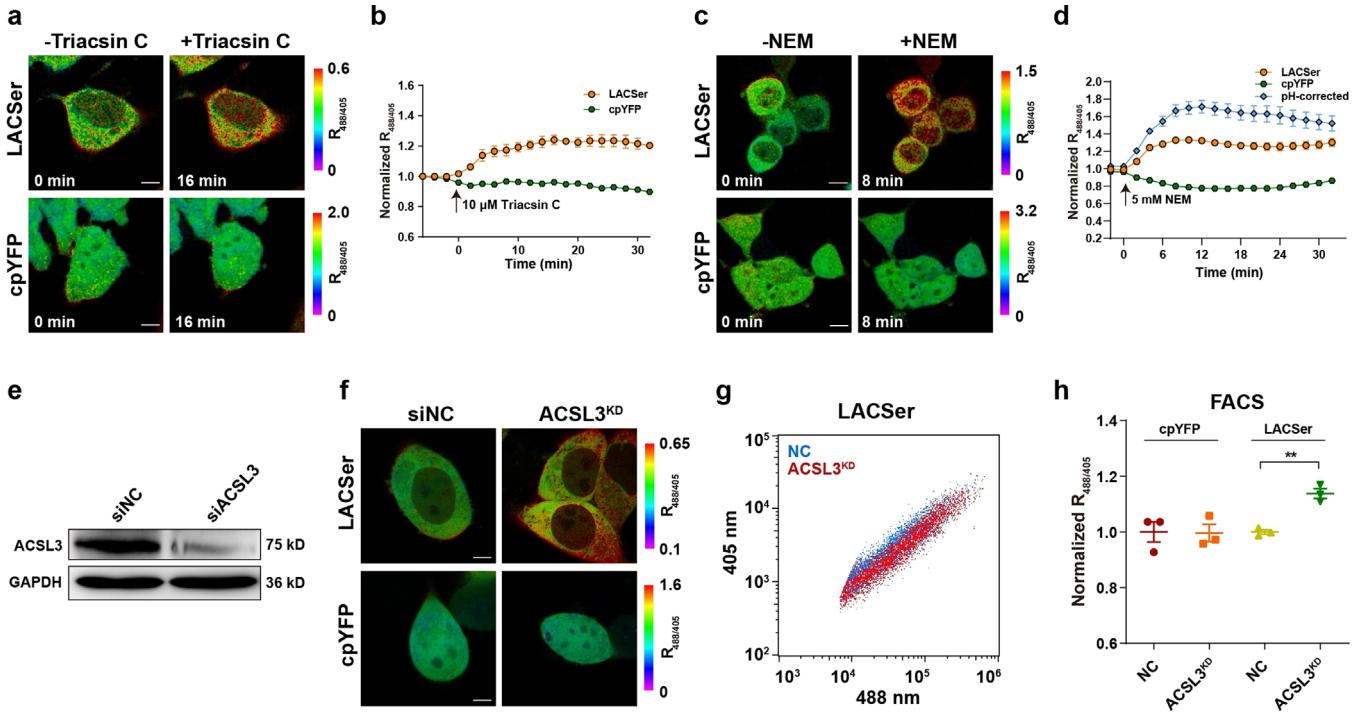

Figure 4. The LCACoAs level decreased upon impairment of ACSL enzyme function. a, b) Fluorescent images (a) and time course of $R_{488/405}$ fluorescent signal changes (b) of HEK293T cells expressing LACSer or free cpYFP in response to Triacsin C, a competitive inhibitor of ACSLs, measured by confocal microscopy. For fluorescent images, the experiment was repeated with three cultures; similar results were obtained each time. Scale bar: 5 μm. For the time course of $R_{488/405}$ fluorescence signal changes, data are presented as the mean ± SEM (LACSer: $n = 13$ cells from three cultures; cpYFP: $n = 10$ cells from three cultures). c, d) Fluorescent images (c) and time course of $R_{488/405}$ fluorescent signal changes (d) of HEK293T cells expressing LACSer or free cpYFP in response to NEM, a covalent inhibitor of ACSLs, measured by confocal microscopy. The blue solid line represents the fluorescence response of LACSer corrected for pH effects. For fluorescent images, the experiment was repeated with three cultures; similar results were obtained each time. Scale bar: 10 μm. For the time course of $R_{488/405}$ fluorescence signal changes, data are presented as the mean ± SEM (LACSer: $n = 20$ cells from three cultures; cpYFP: $n = 17$ cells from three cultures). e) Immunoblotting-based analysis for the efficiency of siRNA-mediated knockdown of ACSL3 ($ACSL3^{KD}$) in HEK293T cells, relative to GAPDH or scramble control. f) Fluorescent images of $ACSL3^{KD}$ or scramble RNA control (siNC) cells expressing LACSer or free cpYFP. The experiment was repeated with two cultures; similar results were obtained both times. Scale bar: 5 μm. g, h) Averaged $R_{488/405}$ fluorescent signal changes of LACSer or free cpYFP in $ACSL3^{KD}$ HEK293T cells, measured by flow cytometry. Each point represents the mean of three replicates and the error bars indicate the SEM. Negative control, HEK293T cells transfected with scramble siRNA. $^{**}P < 0.01$, unpaired t-test.

ACSL3 was knocked down, the $R_{488/405}$ fluorescent signal increased by about 15% relative to the scramble siRNA (negative) control, revealing a decrease in intracellular LCACoAs content; no significant change was observed in cells co-expressing cpYFP and the ACSL3 knockdown construct (Figure 4f). We observed similar fluorescent changes in HEK293T cells that were analyzed by flow cytometry (Figure 4g and h). HPLC-MS confirmed that the knockdown of ACSL3 caused a significant reduction in the levels of LCACoA in HEK293T cells (Figure S9g). Thus, use of our LACSer sensor enabled dynamic sensing and reporting of the biological impacts of ACSL3 knockdown on lipid metabolism.

We also tested whether LACSer can sense and report changes in LCACoA levels in the mitochondrial matrix of HEK293T cells using the aforementioned mito-LACSer variant. Upon treatment of mito-LACSer expressing HEK293T cells with ACSL inhibitors, there was an increased the $R_{488/405}$ fluorescent signal from mitochondria (Figure 5a–d), indicating the anticipated reduction in mitochondrial LCACoAs content. These results establish that LACSer can be used as a sensor for real-time monitoring of mitochondrial LCACoAs dynamics, and also confirm that ACSLs can regulate the level of LCACoAs in mitochondria.

ACBP is an approximately 10 kDa protein that binds LCACoAs with high specificity and affinity ($K_d \approx 1$–10 nM), but does not bind free fatty acids or acyl carnitine, suggesting that ACBP is one of the major carriers of acyl-CoA in cells. Studies have confirmed that ACBP controls the transport of LCACoAs into mitochondria, thereby influencing the levels of LCACoA in mitochondria.[16] However, the current methods for studying the function of ACBP cannot achieve real-time monitoring of mitochondria. We therefore explored use of LACSer to observe dynamic changes in the spatio-temporal distribution of LCACoAs in the cytoplasm and in mitochondria upon experimental modulation of ACBP expression levels.

First, we knocked down ACBP by siRNA in HEK293T cells (Figure 6a) and found that the cytoplasmic fluorescent signal was reduced by about 30% in both flow cytometry and microscopy analyses (Figure 6b–d). By contrast, the fluorescent signal of mitochondrial LACSer increased by about 25%

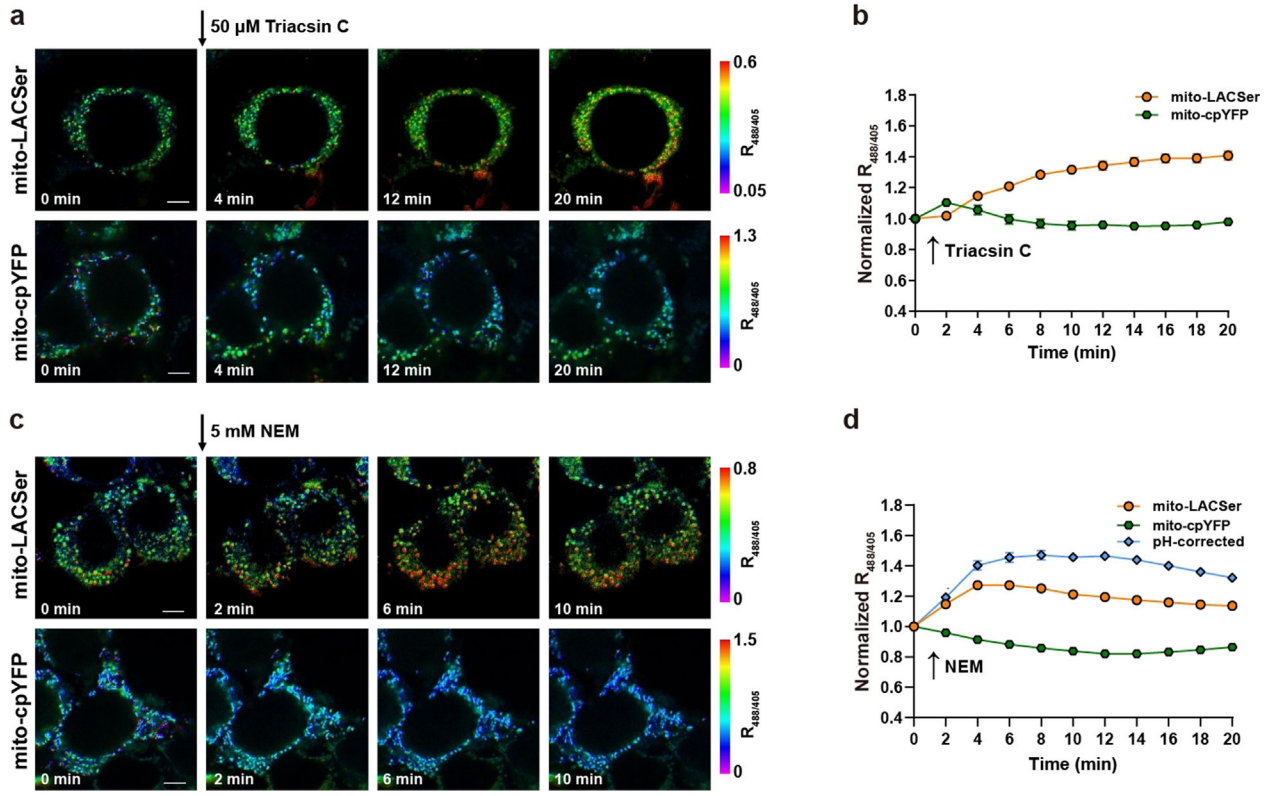

Figure 5. Mitochondrial LCACoA levels are sensitive to ACSL inhibitors. a) Spatiotemporally resolved changes in the ratiometric fluorescence of mito-LACSer or mito-cpYFP in sequential frames in response to 50 μM Triacsin C in HEK293T cells. Images are pseudo-color, with the ratio of fluorescence excited at 488 nm and 405 nm. The experiment was repeated with three cultures; similar results were obtained each time. Scale bar: 5 μm. b) Kinetics of responses of mitochondrial LACSer and cpYFP fluorescence excited at 488 nm and 405 nm in HEK 293T cells treated with 50 μM Triacsin C. Data are presented as the mean ± SEM (mito-LACSer: $n=11$ cells from three cultures; mito-cpYFP: $n=7$ cells from three cultures). c) Spatiotemporally resolved changes in the ratiometric fluorescence of mito-LACSer or mito-cpYFP in sequential frames in response to 5 mM NEM in HEK293T cells. Images are pseudo-color, with the ratio of fluorescence excited at 488 nm and 405 nm. The experiment was repeated with three cultures; similar results were obtained each time. Scale bar: 5 μm. d) Kinetics of responses of mitochondrial LACSer and cpYFP fluorescence excited at 488 nm and 405 nm in HEK293T cells treated with 5 mM NEM. The blue solid line represents the fluorescence response of mito-LACSer corrected for pH effects. Data are presented as the mean ± SEM (mito-LACSer: $n=12$ cells from three cultures; mito-cpYFP: $n=12$ cells from three cultures).

(Figure 6e and f). These results indicate that compared to scramble control cells, the free LCACoA levels were higher in cytoplasm upon ACBP knockdown but lower in mitochondria, suggesting reduced ACBP-mediated transport of LCACoAs from the cytoplasm to mitochondria (Figure 6g). In summary, these results confirm that ACBP can maintain cytosolic LCACoA levels and regulate the mitochondrial distribution of LCACoAs.

Conclusion

We developed, characterized, and scientifically deployed LACSer, an innovative genetically encoded fluorescent sensor for in vivo detection of LCACoAs. LACSer shows excellent selectivity and sensitivity (submicromolar) for LCACoA binding, and LACSer's fluorescence ratio is highly sensitive to intracellular LCACoA levels. Thus, LACSer achieves dynamic detection of LCACoAs in cells and even subcellular organelles (cytoplasm vs. mitochondria), establishing its utility for investigations of fine-scale LCACoAs distributions in human cells in real time. We successfully obtained empirical evidence from living human cells in support of previous findings based on indirect detection methods, specifically regarding function of ACSLs in determining intracellular contents of LCACoAs and the function of ACBPs in facilitating mitochondrial import of LCACoAs, thereby supporting fatty acid β-oxidation and ATP production.

The pH stability of a biosensor is relevant because the pH fluctuates in cells, in various organelles, and in the course of various physiological processes. When working with a pH-sensitive probes, these fluctuations can generate pH bias in their readouts. To manage potential pH bias, we applied a previously reported simple calibration strategy for the approximate removal of pH bias from biosensor signals.[29] This method was suitable because of the similar pH sensitivity we detected for LACSer and cpYFP; we normalize LACSer fluorescence based on the cpYFP fluorescence data measured in parallel experiments. Owing to this pH correction, LACSer is suitable for measuring dynamic changes in intracellular free LCACoA levels in various cellular pH contexts.

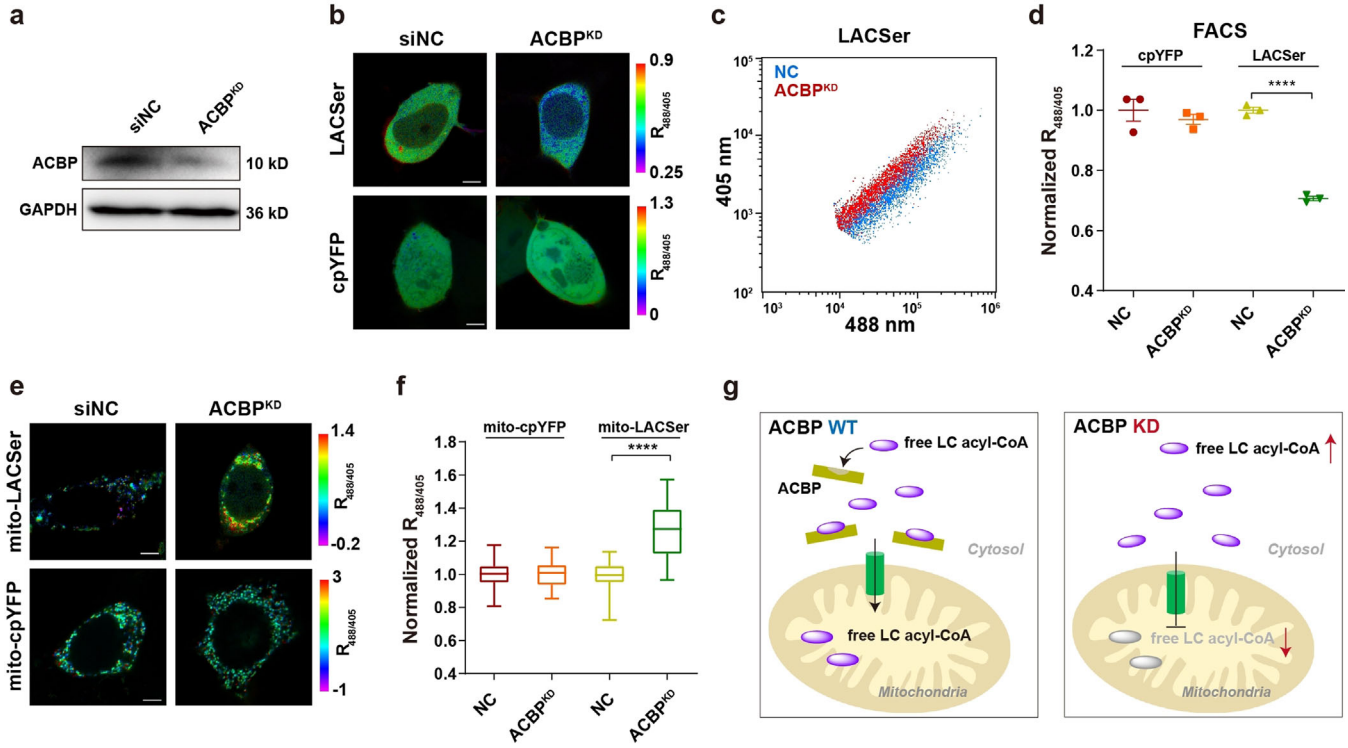

Figure 6. ACBP expression differentially impacts mitochondrial vs. cytosolic LCACoA levels. a) Immunoblotting-based analysis for the efficiency of ACBP-knockdown (ACBP^{KD}) in HEK293T cells. b) Fluorescent images of ACBP^{KD} or scramble RNA control (siNC) HEK293T cells expressing LACSer or free cpYFP. The experiment was repeated with two cultures; similar results were obtained each time. Scale bar: 5 μm. c, d) Averaged $R_{488/405}$ fluorescent signal changes of LACSer or free cpYFP in ACBP^{KD} HEK293T cells, measured by flow cytometry. Each point represents the mean of three replicates and the error bars indicate the SEM. e, f) Fluorescent images (e) and averaged $R_{488/405}$ fluorescent signal changes (f) of mito-LACSer or mito-cpYFP in ACBP^{KD} HEK293T cells, measured by confocal microscopy. For fluorescent images, the experiment was repeated with two cultures; similar results were obtained each time. Scale bar: 5 μm. For the $R_{488/405}$ fluorescence signal change: for ACBP^{KD}, mito-LACSer: $n=48$ cells from two cultures; mito-cpYFP: $n=61$ cells from two cultures; for negative control (NC), mito-LACSer: $n=51$ cells from two cultures; mito-cpYFP: $n=65$ cells from two cultures). In (b) to (f), negative control (NC) indicates HEK293T cells transfected with scramble siRNA. ****$P<0.0001$, unpaired t-test. g) Schematic diagram for binding of LCACoAs with ACBP and subsequent transport into mitochondria.

Given its excellent sensitivity, specificity, and photostability, LACSer can clearly support investigations of LCACoAs with high spatiotemporal resolution. Looking towards future iterations of this sensor and associated detection methods, it may be possible to engineer LACSer sensor variants that are specifically localized and/or anchored to additional subcellular compartments or structures, via fusion of appropriate signal peptides or binding/interaction domains. As demonstrated in our LACSer-based mitochondrial investigations, the capacity to monitor the intracellular synthesis/utilization of LCACoAs opens the door for previously inaccessible experiments that could for example delineate the energy production vs. singaling functions of LCACoAs, for example to distinguish specific impacts of dynamic substrate pools on a potentially very large number of protein-lipidation-based signaling events.

It may also be possible to further tune the specificity of LACSer and structurally similar iterations of these sensors to for instance specifically monitor myristoyl-CoA and palmitoyl-CoA, again in a variety of cellular and subcellular contexts. Given the known preferences of FadR for C12-C20 LCACoAs,[18] it may even be possible to further develop the LACSer concept as a general platform for in vivo detection of diverse lipid molecules. Success in such efforts would not only help deepen our basic understanding about lipid metabolism, it could dramatically expand our biotechnological capacities for metabolic engineering and for biomedical screening applications in drug development and even clinical imaging.

Acknowledgements

This work supported by the National Basic Research Foundation of China (No. 2017YFA0505202 to J.W. and G.F.Y.), the National Natural Science Foundation of China (91853107 to J.W.). J.W. also thanks the Youth Thousand-Talents Program of China for support.

Conflict of interest

The authors declare no conflict of interest.

Keywords: biosensors · cell imaging · LC acyl-CoA metabolism · long-chain fatty acyl-CoA · protein engineering

[1] N. J. Færgeman, J. Knudsen, *Biochem. J.* **1997**, *323*, 1 – 12.
[2] A. Yamashita, Y. Hayashi, N. Matsumoto, Y. Nemoto-Sasaki, S. Oka, T. Tanikawa, T. Sugiura, *Biology* **2014**, *3*, 801 – 830.
[3] R. Tidhar, A. H. Futerman, *Biochim. Biophys. Acta Mol. Cell Res.* **2013**, *1833*, 2511 – 2518.
[4] A. Kihara, *J. Biochem.* **2012**, *152*, 387 – 395.
[5] a) C. C. DiRusso, A. K. Metzger, T. L. Heimert, *Mol. Microbiol.* **1993**, *7*, 311 – 322; b) B. R. Sabari, D. Zhang, C. D. Allis, Y. Zhao, *Nat. Rev. Mol. Cell Biol.* **2017**, *18*, 90 – 101.
[6] S. Majumdar, M. W. Rossi, T. Fujiki, W. A. Phillips, S. Disa, C. F. Queen, R. B. Johnston, O. M. Rosen, B. E. Corkey, H. M. Korchak, *J. Biol. Chem.* **1991**, *266*, 9285 – 9294.
[7] C. Zhang, A. Li, S. Gao, X. Zhang, H. Xiao, *PLoS One* **2011**, *6*, e21233.
[8] K. S. Hamming, M. J. Riedel, D. Soliman, L. C. Matemisz, N. J. Webster, G. J. Searle, P. E. MacDonald, P. E. Light, *Mol. Endocrinol.* **2008**, *22*, 2293 – 2306.
[9] a) O. Larsson, J. T. Deeney, R. Bränström, P. O. Berggren, B. E. Corkey, *J. Biol. Chem.* **1996**, *271*, 10623 – 10626; b) M. J. Riedel, I. Baczkó, G. J. Searle, N. Webster, M. Fercho, L. Jones, J. Lang, J. Lytton, J. R. Dyck, P. E. Light, *EMBO J.* **2006**, *25*, 4605 – 4614.
[10] G. R. Wagner, D. P. Bhatt, T. M. O'Connell, J. W. Thompson, L. G. Dubois, D. S. Backos, H. Yang, G. A. Mitchell, O. R. Ilkayeva, R. D. Stevens, P. A. Grimsrud, M. D. Hirschey, *Cell Metab.* **2017**, *25*, 823 – 837.e828.
[11] R. N. Hannoush, J. Sun, *Nat. Chem. Biol.* **2010**, *6*, 498 – 506.
[12] B. Chen, Y. Sun, J. Niu, G. K. Jarugumilli, X. Wu, *Cell Chem. Biol.* **2018**, *25*, 817 – 831.
[13] M. Hundt, H. Tabata, M. S. Jeon, K. Hayashi, Y. Tanaka, R. Krishna, L. De Giorgio, Y. C. Liu, M. Fukata, A. Altman, *Immunity* **2006**, *24*, 513 – 522.
[14] a) T. Harayama, H. Riezman, *Nat. Rev. Mol. Cell Biol.* **2018**, *19*, 281 – 296; b) X. Han, *Nat. Rev. Endocrinol.* **2016**, *12*, 668 – 679; c) J. Zha, S. Weiler, K. J. Oh, M. C. Wei, S. J. Korsmeyer, *Science* **2000**, *290*, 1761 – 1765.
[15] a) J. S. Yount, B. Moltedo, Y.-Y. Yang, G. Charron, T. M. Moran, C. B. López, H. C. Hang, *Nat. Chem. Biol.* **2010**, *6*, 610 – 614; b) H. Jiang, S. Khan, Y. Wang, G. Charron, B. He, C. Sebastian, J. Du, R. Kim, E. Ge, R. Mostoslavsky, H. C. Hang, Q. Hao, H. Lin, *Nature* **2013**, *496*, 110 – 113; c) M. E. Linder, R. J. Deschenes, *Nat. Rev. Mol. Cell Biol.* **2007**, *8*, 74 – 84.
[16] a) J. Bi, P. Mischel, *Cell Metab.* **2019**, *30*, 229 – 230; b) C. Duman, K. Yaqubi, A. Hoffmann, A. A. Acikgöz, A. Korshunov, M. Bendszus, C. Herold-Mende, H.-K. Liu, J. Alfonso, *Cell Metab.* **2019**, *30*, 274 – 289.e275.
[17] C. Brocker, C. Carpenter, D. W. Nebert, V. Vasiliou, *Hum. Genomics* **2010**, *4*, 411 – 420.
[18] E. Soupene, F. A. Kuypers, *Exp. Biol. Med.* **2008**, *233*, 507 – 521.
[19] D. Neess, S. Bek, H. Engelsby, S. F. Gallego, N. J. Færgeman, *Prog. Lipid Res.* **2015**, *59*, 1 – 25.
[20] T. J. Grevengoed, E. L. Klett, R. A. Coleman, *Annu. Rev. Nutr.* **2014**, *34*, 1 – 30.
[21] a) L. Abrankó, G. Williamson, S. Gardner, A. Kerimi, *J. Chromatogr. A* **2018**, *1534*, 111 – 122; b) C. Magnes, F. M. Sinner, W. Regittnig, T. R. Pieber, *Anal. Chem.* **2005**, *77*, 2889 – 2894; c) D. Morin-Rivron, N. Christinat, M. Masoodi, *Rapid Commun. Mass Spectrom.* **2017**, *31*, 344 – 350.
[22] V. V. Belousov, A. F. Fradkov, K. A. Lukyanov, D. B. Staroverov, K. S. Shakhbazov, A. V. Terskikh, S. Lukyanov, *Nat. Methods* **2006**, *3*, 281 – 286.
[23] C. C. DiRusso, V. Tsvetnitsky, P. Højrup, J. Knudsen, *J. Biol. Chem.* **1998**, *273*, 33652 – 33659.
[24] D. M. F. van Aalten, C. C. DiRusso, J. Knudsen, *EMBO J.* **2001**, *20*, 2041 – 2050.
[25] J. S. Marvin, E. R. Schreiter, I. M. Echevarría, L. L. Looger, *Proteins Struct. Funct. Bioinf.* **2011**, *79*, 3025 – 3036.
[26] D. C. Nadler, S.-A. Morgan, A. Flamholz, K. E. Kortright, D. F. Savage, *Nat. Commun.* **2016**, *7*, 12266.
[27] E. C. Greenwald, S. Mehta, J. Zhang, *Chem. Rev.* **2018**, *118*, 11707 – 11794.
[28] R. Bizzarri, M. Serresi, S. Luin, F. Beltram, *Anal. Bioanal. Chem.* **2009**, *393*, 1107.
[29] a) Y. Zhao, J. Jin, Q. Hu, H. M. Zhou, J. Yi, Z. Yu, L. Xu, X. Wang, Y. Yang, J. Loscalzo, *Cell Metab.* **2011**, *14*, 555 – 566; b) Y. Zhao, Q. Hu, F. Cheng, N. Su, A. Wang, Y. Zou, H. Hu, X. Chen, H. M. Zhou, X. Huang, K. Yang, Q. Zhu, X. Wang, J. Yi, L. Zhu, X. Qian, L. Chen, Y. Tang, J. Loscalzo, Y. Yang, *Cell Metab.* **2015**, *21*, 777 – 789; c) X. A. Cambronne, M. L. Stewart, D. Kim, A. M. Jones-Brunette, R. K. Morgan, D. L. Farrens, M. S. Cohen, R. H. Goodman, *Science* **2016**, *352*, 1474 – 1477; d) Y. Zhao, A. Wang, Y. Zou, N. Su, J. Loscalzo, Y. Yang, *Nat. Protoc.* **2016**, *11*, 1345 – 1359.
[30] J. G. Boylan, J. A. Hamilton, *Biochemistry* **1992**, *31*, 557 – 567.
[31] D. G. Mashek, L. O. Li, R. A. Coleman, *Future Lipidol.* **2007**, *2*, 465 – 476.
[32] J.-H. Kim, T. M. Lewin, R. A. Coleman, *J. Biol. Chem.* **2001**, *276*, 24667 – 24673.

Manuscript received: February 3, 2021
Revised manuscript received: March 14, 2021
Accepted manuscript online: April 10, 2021
Version of record online: ■■ ■■, ■■■■

Research Articles

Biosensors

W. B. Wang, Q. P. Wei, J. Y. Zhang, M. Q. Zhang, C. C. Wang, R. Y. Qu, Y. Wang, G. F. Yang,* J. Wang* _____ ▮▮▮▮–▮▮▮▮

A Ratiometric Fluorescent Biosensor Reveals Dynamic Regulation of Long-Chain Fatty Acyl-CoA Esters Metabolism

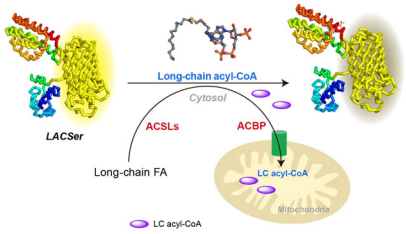

LACSer, a genetically encoded long-chain acyl-CoA fluorescence sensor, generates a specific fluorescence response to long-chain acyl-CoA, and can be used for the ratiometric quantification of long-chain acyl-CoA in cells and subcellular structures. The effects of ACSL and ACBP on the biosynthesis, transport, and downstream metabolism of long-chain acyl-CoA can be studied.